Relaxin Family Peptide Receptor-1 Protects against Airway Fibrosis during Homeostasis But Not against Fibrosis Associated with Chronic Allergic Airways Disease

Chrishan S. Samuel,* Simon G. Royce,* Bin Chen, Huifang Cao, Jan A. Gossen, Geoffrey W. Tregear, and Mimi L. K. Tang

Howard Florey Institute (C.S.S., H.C., G.W.T.) and Departments of Biochemistry and Molecular Biology (C.S.S., G.W.T.) and Paediatrics (M.L.K.T.), University of Melbourne, Victoria 3010, Australia; Allergy and Immune Disorders (S.G.R., B.C., M.L.K.T.), Murdoch Children's Research Institute, and Department of Allergy and Immunology (S.G.R., B.C., M.L.K.T.), Royal Children's Hospital, Parkville, Victoria 3052, Australia; and Target Discovery Department (J.A.G.), Schering-Plough Corporation, 5340 BH Oss, The Netherlands

Endogenous relaxin has recently been demonstrated to protect the airway/lung against age-related fibrosis and against inflammation-associated airway fibrosis in animal models of allergic airways disease (AAD). In the current study, we examined the contribution of the primary relaxin receptor, relaxin family peptide receptor-1 (RXFP1), in mediating these effects of relaxin. Lung tissues from healthy aging RXFP1 gene-knockout (Rxfp1$^{-/-}$) and wild-type (Rxfp1$^{+/+}$) mice and from 8- to 10-wk-old Rxfp1$^{-/-}$ and Rxfp1$^{+/+}$ mice subjected to a mouse model of AAD were assessed for various markers of airway fibrosis and remodeling. Male and female Rxfp1$^{-/-}$ mice demonstrated an age-related progression of airway/lung fibrosis. Saline-treated Rxfp1$^{-/-}$ mice had significantly increased myofibroblast differentiation and lung collagen deposition (both $P < 0.05$), decreased matrix metalloproteinase (MMP)-9 expression and activity ($P < 0.05$), but equivalent levels of MMP-2 and tissue inhibitor of metalloproteinases (TIMPs) to that measured in saline-treated Rxfp1$^{+/+}$ mice. As expected, ovalbumin (OVA)-treated Rxfp1$^{+/+}$ mice developed markedly increased lung myofibroblast differentiation and collagen deposition (both $P < 0.01$ vs saline-treated Rxfp1$^{+/+}$ mice), significantly decreased lung MMP-2 and MMP-9 expression and activity and increased TIMP-1 expression (all $P < 0.05$ *vs.* respective measurements from saline-treated Rxfp1$^{+/+}$ mice). Surprisingly, however, OVA-treated Rxfp1$^{-/-}$ animals had equivalent levels of airway fibrosis and gelatinase activity but increased TIMP-1 expression ($P < 0.05$) compared with OVA-treated Rxfp1$^{+/+}$ mice. These combined findings demonstrate that RXFP1 is involved in mediating relaxin's effects on airway fibrosis during homeostasis but not during inflammation-induced fibrosis associated with chronic AAD. (***Endocrinology*** **150: 1495–1502, 2009)**

Originally discovered as a reproductive hormone (1–3), relaxin is now emerging as an important endocrine and paracrine factor which protects several organs, including the lung, from collagen accumulation leading to fibrosis (4). Relaxin-deficient (*Rln*$^{-/-}$) mice demonstrate an age-related progression of airway/lung fibrosis (5) and also manifest exaggerated airway fibrosis when subjected to ovalbumin (OVA)-induced airway inflammation (6, 7), confirming relaxin's status as an endogenous regulator of collagen turnover in health and disease. Moreover, prolonged relaxin deficiency (over 12 months) leads to structural and functional changes in the mouse lung that mimic those observed in models of allergic airways disease (AAD), specifically collagen deposition in the subepithelial basement membrane region and submucosa (5, 7), and airway hyperresponsiveness (AHR; a measure of airway dysfunction) (7). Based on these studies and those examining the effects of exogenous re-

ISSN Print 0013-7227 ISSN Online 1945-7170
Printed in U.S.A.
Copyright © 2009 by The Endocrine Society
doi: 10.1210/en.2008-1062 Received July 17, 2008. Accepted October 20, 2008.
First Published Online October 30, 2008
* C.S.S. and S.G.R. contributed equally to this work.

Abbreviations: AAD, Allergic airways disease; AHR, airway hyperresponsiveness; BAL, bronchoalveolar lavage; LGR, leucine-rich repeat containing G protein-coupled receptor; MCh, methacholine; MMP, matrix metalloproteinase; OVA, ovalbumin; RXFP1, relaxin family peptide receptor-1; α-SMA, α-smooth muscle actin; TIMP-1, tissue inhibitor of metalloproteinase.

Downloaded from endo.endojournals.org by on May 31, 2010

laxin therapy in models of lung disease (8–10), it is proposed that relaxin's protective effects are mediated via its ability to stimulate matrix metalloproteinase (MMP)-induced collagen breakdown and inhibit TGF-β1-induced collagen production.

The relaxin receptor was recently discovered as a leucine-rich repeat containing G protein-coupled receptor (LGR) (11) and shown to be expressed in the human (11) and mouse (5) lung. Initially discovered as LGR7, this receptor has now been reclassified as relaxin family peptide receptor-1 (RXFP1) and belongs to a subgroup (type C) of the family of LGRs that include receptors for FSH, LH, and TSH (12). The finding of phenotypic similarities in several reproductive organs of pregnant female (13, 14) and developing male (15) $Rln^{-/-}$ and RXFP1-deficient ($Rxfp1^{-/-}$) (16, 17) mice indicated that relaxin can induce some of its biological effects via RXFP1 *in vivo*. Additionally, the effects of relaxin in protecting the aging lung from the progression of collagen accumulation are mediated at least in part through the RXFP1 receptor, because both $Rln^{-/-}$ (5) and $Rxfp1^{-/-}$ (17) mice undergo an age-related progression of pulmonary fibrosis.

Importantly though, RXFP1 deficiency appeared to have a greater impact on the age-related progression of pulmonary fibrosis, because $Rxfp1^{-/-}$ mice underwent increases in lung collagen accumulation as early as 1 month of age (17), whereas fibrosis in the airway/lung was evident in $Rln^{-/-}$ mice only by 6–9 months of age (5), suggesting that additional ligands other than relaxin may also signal through RXFP1. Indeed, other relaxin peptides such as H3 relaxin and its mouse equivalent, relaxin-3, have also been shown to bind and activate RXFP1 (18). Furthermore, a recent study has demonstrated that relaxin can act as a ligand for the glucocorticoid receptor (19). These findings suggest that relaxin is not the sole ligand for RXFP1 and that RXFP1 is not the sole receptor for relaxin, highlighting the complexity of relaxin physiology.

In the current study, we sought to delineate whether the protective effects of relaxin in the lung of aging mice (5) and mice subjected to AAD (6) were mediated through its native receptor, RXFP1. We employed a well-characterized murine model of chronic AAD, which mimics several features of human asthma (20), to RXFP1 wild-type ($Rxfp1^{+/+}$) and $Rxfp1^{-/-}$ mice and compared our findings to that previously obtained from $Rln^{-/-}$ mice subjected to the same model (6). The relationship between airway fibrosis, other structural changes of airway remodeling, and AHR was also examined in the model of AAD.

Materials and Methods

Animals

All male and female $Rxfp1^{+/+}$ and $Rxfp1^{-/-}$ littermate mice used in this study were generated from RXFP1-heterozygous ($Rxfp1^{+/-}$) parents, as described previously (16).

For the AAD studies, 8- to 10-wk-old mice were used to match the age at which $Rln^{+/+}$ and $Rln^{-/-}$ were subjected to the chronic model of AAD (6) and were housed and fed in a controlled environment, as described before (5, 6). These experiments were approved by the Howard Florey Institute and Royal Children's Hospital Animal Ethics Committees, which adhere to the Australian Code of Practice for the care and use of laboratory animals for scientific purposes.

OVA-induced allergic airways disease model

The 9-wk OVA-induced model of AAD, described previously (6, 20) was applied to $Rxfp1^{+/+}$ and $Rxfp1^{-/-}$ littermate mice. Eight- to 10-wk-old male (n = 18) and female (n = 19) mice were sensitized with an ip injection of 10 μg grade V OVA (Sigma Chemical Co., St. Louis, MO) and 1 mg aluminum potassium sulfate (Sigma) in 0.5 ml saline on d 0 and 14. Mice were then challenged 3 d/wk for 6 wk (from d 21–63) with an aerosol of 2.5% (wt/vol) OVA in saline for 30 min. Aerosol challenge was carried out on groups of up to 16 mice in a whole-body inhalation exposure system attached to an ultrasonic nebulizer (NE-U07; Omron Corp., Tokyo, Japan) with an output of 1 ml/min and 1- to 5-μm particle size. Saline-treated (control) male (n = 16) and female (n = 16) mice received an ip injection of saline alone (0.5 ml) on d 0 and 14 and were challenged with saline aerosols.

Analysis of AHR

Methacholine (MCh)-induced airway reactivity was assessed 24 h after the final OVA or saline aerosol challenge by invasive plethysmography (Buxco Electronics, Troy, NJ), as described previously (6, 7, 20).

Determination of OVA-specific IgE levels

To validate the model of AAD and confirm that the mice were adequately sensitized to OVA, serum levels of OVA-specific IgE, obtained 24 h after the final OVA or saline aerosol challenge, were determined by ELISA, as described previously (6, 7, 20, 21).

Bronchoalveolar lavage (BAL)

To assess airway inflammation, the influx of leukocytes into the airway lumen was examined. BAL was performed on anesthetized mice, 24 h after the final OVA or saline aerosol challenge, as described before (6, 7, 20, 21). Total viable cells were determined in a hemocytometer using trypan blue exclusion and the results expressed as total cell number $\times 10^4$.

Tissue collection

For the aging studies, lung tissues were isolated from male and female $Rxfp1^{+/+}$ and $Rxfp1^{-/-}$ littermate mice (n = 5–8 per gender, genotype, and time point) at 2, 4, and 8 months of age. For the AAD studies, lung tissues were isolated from male and female $Rxfp1^{+/+}$ and $Rxfp1^{-/-}$ littermate mice (n = 6–10 per gender and genotype). All tissues were weighed (total lung weight) and then separated into individual lobes for histological and biochemical analyses, as detailed below.

Lung histopathology and morphometric analysis of structural changes

The right lung lobe and trachea were fixed in 10% neutral buffered formalin for approximately 18–24 h and routinely processed. Serial 5-μm sections taken from 100-μm intervals of each tissue were stained with hematoxylin and eosin (for morphological assessment of peribronchial inflammation), Masson trichrome (for assessment of subepithelial fibrosis) and Alcian blue periodic acid Schiff (for assessment of goblet cells). Morphometric analysis of tissues was performed as described before (6, 7, 20).

Hydroxyproline analysis of lung collagen

A portion of each lung from untreated (aging) $Rxfp1^{+/+}$ and $Rxfp1^{-/-}$ mice and from saline- and OVA-treated $Rxfp1^{+/+}$ and $Rxfp1^{-/-}$ mice was treated as described previously (22, 23) for hydroxyproline determination. Hydroxyproline values were then converted to collagen content by multiplying by a factor of 6.94 (based on hydroxyproline representing approximately 14.4% of the amino acid composition of collagen in most mammalian tissues (24) and expressed as the relative ratio of the collagen content in saline-treated $Rxfp1^{+/+}$ mice, which was expressed as 1.

Downloaded from endo.endojournals.org by on May 31, 2010

SDS-PAGE of interstitial lung collagens

The insoluble interstitial matrix collagens (I, III, and V) were extracted from equivalent lung portions of saline- and OVA-treated *Rxfp1*$^{+/+}$ and *Rxfp1*$^{-/-}$ mice, as described before (23). The maturely cross-linked collagen was extracted by limited pepsin digestion (enzyme/substrate ratio, 1:10) for 24 h at 4 C, before pepsin-digested extracts were analyzed by SDS-PAGE (23). Samples were run on 5% acrylamide gels containing 3.5% stacking gels. Interrupted electrophoresis with delayed reduction of the disulfide bonds of type III collagen was used to separate the α1(III) from the α1(I) chains (25). The gels were stained overnight at 4 C with 0.1% Coomassie brilliant blue R-250, before being destained with 30% methanol containing 7% acetic acid and then dried and photographed. Densitometry of the type I collagen [α1(I) and α2(I)] chains was performed using a Bio-Rad (Richmond, CA) GS710 calibrated imaging densitometer and Quantity-One software (Bio-Rad). The relative OD collagen I in each group was then expressed as a ratio of that in saline-treated *Rxfp1*$^{+/+}$ mice, which was expressed as 1.

Western blot analysis of α-smooth muscle actin (α-SMA)

To determine whether the effects of RXFP1 deficiency on airway collagen, in the absence or presence of the AAD model, were mediated via regulation of myofibroblast differentiation, Western blot analysis of α-SMA (a well characterized marker of myofibroblasts) was performed. Total protein was extracted from tissues with the Trizol reagent (according to the manufacturer's instructions; Life Technologies, Gaithersburg, MD) and quantitated by the Bio-Rad dye-binding protein assay. Protein extracts (in 1% sodium dodecyl sulfate; 10 μg total protein/lane) were electrophoresed under nonreducing conditions on 12.5% acrylamide gels, as previously described (26). Western blot analysis was performed with a monoclonal antibody to α-SMA (M0851, 1:1000 dilution; Dako Corp., Carpinteria, CA) overnight and a goat antimouse secondary antibody (1:2000 dilution; Dako) for 2 h. Densitometry of the α-SMA bands was performed as described above. The relative OD α-SMA in each group was then expressed as a ratio of that in saline-treated *Rxfp1*$^{+/+}$ mice, which was expressed as 1.

Gelatin zymography

To determine whether the effects of RXFP1 deficiency on subepithelial collagen, in the absence or presence of the AAD model, were mediated via the regulation of gelatinases MMP-2 (gelatinase-A) and MMP-9 (gelatinase-B), gelatin zymography of lung tissue from each of the groups studied was performed as described before (27). Equal aliquots of the MMP extracts were analyzed on zymogram gels consisting of 7.5% acrylamide and 1 mg/ml gelatin, and the gels were subsequently treated as previously detailed (27). Gelatinolytic activity was quantitated by densitometry (as detailed above) and the relative OD for MMP-2 and -9 in each group expressed as the respective ratio of that in saline-treated *Rxfp1*$^{+/+}$ mice, which was expressed as 1.

Reverse zymography

To determine whether the effects of RXFP1 deficiency on subepithelial collagen, in the absence or presence of the AAD model, were mediated via regulation of the tissue inhibitor of metalloproteinase-1 (TIMP-1) and TIMP-2, reverse zymography of lung tissue from each of the groups studied was performed as detailed elsewhere (28) and compared with purified standards of TIMP-1 and TIMP-2 (Calbiochem, San Diego, CA). Again, TIMP activity was quantitated by densitometry (as detailed above) and the relative OD for TIMP-1 and TIMP-2 in each group expressed as the respective ratio of that in saline-treated *Rxfp1*$^{+/+}$ mice, which was expressed as 1.

Statistical analysis

The results were analyzed using a one-way ANOVA and the Newman-Keuls posttest for multiple comparisons between groups. AHR was analyzed with a two-way ANOVA and the Bonferroni posttest. All data in this paper are presented as the mean ± SEM, with $P < 0.05$ described as statistically significant.

Results

Rxfp1$^{-/-}$ mice demonstrate an age-related progression of airway fibrosis

Lung collagen deposition (the predominant component of lung fibrosis) was progressively increased in both male and female *Rxfp1*$^{-/-}$ mice by 2 and 4 months of age, respectively, and continued to increase until at least 8 months of age compared with that measured in age-matched *Rxfp1*$^{+/+}$ animals (Fig. 1). Lung collagen content was significantly increased in male *Rxfp1*$^{-/-}$ mice by 19, 28, and 35% (all $P < 0.05$) at 2, 4, and 8 months of age, respectively, and in female *Rxfp1*$^{-/-}$ mice by 15 and 18% (all $P < 0.05$) at 4 and 8 months of age, compared with that measured in age-matched *Rxfp1*$^{+/+}$ animals (Fig. 1).

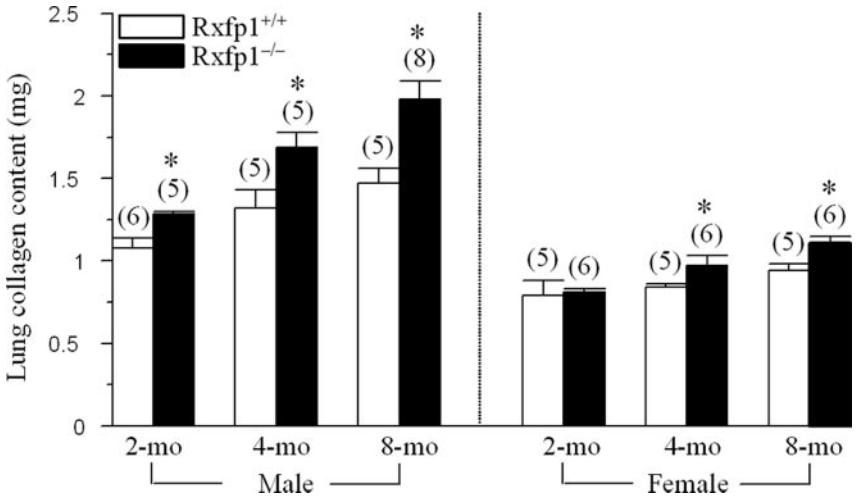

FIG. 1. Total lung collagen content (which was converted from the hydroxyproline values) was measured in aging male and female *Rxfp1*$^{+/+}$ and *Rxfp1*$^{-/-}$ mice, at 2, 4, and 8 months of age. *Numbers in parentheses* represent number of animals per group. *, $P < 0.05$ *vs.* respective values from age-matched/gender-matched *Rxfp1*$^{+/+}$ mice.

Rxfp1$^{+/+}$ and *Rxfp1*$^{-/-}$ mice have normal sensitization and airway inflammation responses to OVA

Serum levels of OVA-specific IgE (Fig. 2A) and BAL cell counts (Fig. 2B) were examined to confirm that *Rxfp1*$^{+/+}$ and *Rxfp1*$^{-/-}$ mice were adequately sensitized to OVA. In each case, no gender-based differences in these parameters were observed, and hence, all results shown are presented as the combined (male and female) data from the four groups studied. Serum levels of OVA-specific IgE in OVA-treated *Rxfp1*$^{-/-}$ mice were equivalent to those of OVA-treated *Rxfp1*$^{+/+}$ animals and were significantly higher ($P < 0.001$) than levels measured in saline-treated control mice, which did not demonstrate detectable OVA-specific IgE levels (Fig. 2A).

Downloaded from endo.endojournals.org by on May 31, 2010

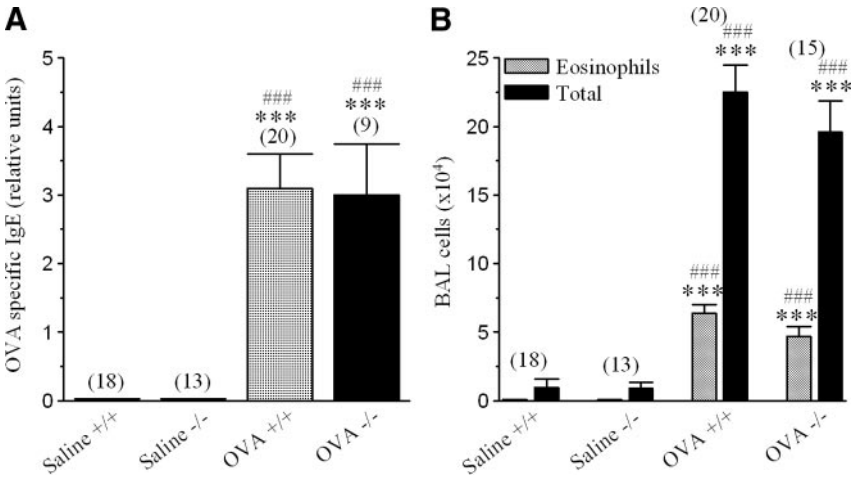

FIG. 2. OVA-specific IgE and BAL cell counts in OVA-sensitized/challenged *Rxfp1*$^{+/+}$ and *Rxfp1*$^{-/-}$ mice. OVA-induced inflammation was assessed by OVA-specific IgE (A) and eosinophil and total BAL cell counts of airway inflammatory cells (B) in saline- and OVA-treated *Rxfp1*$^{+/+}$ and *Rxfp1*$^{-/-}$ mice. Results are presented as the mean ± SE. OVA-specific IgE (relative units) (A) or BAL cells (× 10^4) (B). *Numbers in parentheses* represent number of animals per group. ***, $P < 0.001$ *vs.* respective values from saline-treated *Rxfp1*$^{+/+}$ mice; ###, $P < 0.001$ *vs.* respective values from saline-treated *Rxfp1*$^{-/-}$ mice.

Additionally, both *Rxfp1*$^{+/+}$ and *Rxfp1*$^{-/-}$ mice demonstrated increased total (both $P < 0.001$) and differential (both $P < 0.001$) BAL cell counts after OVA sensitization treatment, compared with numbers obtained from saline-treated control animals (Fig. 2B). There was no significant difference in total cell counts (Fig. 2B) or eosinophil (Fig. 2B), neutrophil, monocyte, and lymphocyte cell counts between OVA-treated *Rxfp1*$^{+/+}$ and *Rxfp1*$^{-/-}$ mice. These combined data demonstrated that *Rxfp1*$^{+/+}$ and *Rxfp1*$^{-/-}$ mice were able to mount similar IgE and airway inflammation responses after OVA sensitization.

Analysis of collagen deposition, collagen subtypes, and myofibroblast differentiation in the airways/lung of *Rxfp1*$^{+/+}$ and *Rxfp1*$^{-/-}$ mice

Lung tissues from saline- or OVA-treated *Rxfp1*$^{+/+}$ and *Rxfp1*$^{-/-}$ mice were analyzed by quantitative biochemical means and by histology/morphometry to determine the relative amount and distribution of collagen deposition, respectively. In each case, no gender-based differences in collagen deposition were observed, and hence, all results shown are presented as the combined (male and female) data from the four groups studied. Lung tissue sections from saline-treated *Rxfp1*$^{+/+}$ mice stained with Masson trichrome showed minimal collagen deposition in the airway and lung parenchyma (Fig. 3A), whereas saline-treated *Rxfp1*$^{-/-}$ mice demonstrated a modest increase in collagen deposition in the airways (Fig. 3B). OVA treatment of *Rxfp1*$^{+/+}$ (Fig. 3C) and *Rxfp1*$^{-/-}$ (Fig. 3D) mice resulted in a markedly increased collagen staining within the airways, when compared with the respective saline-treated controls. Of note, collagen staining was equivalent in OVA-treated *Rxfp1*$^{+/+}$ and *Rxfp1*$^{-/-}$ mice. The increase in collagen staining observed in saline-treated *Rxfp1*$^{-/-}$ mice and OVA-treated animals was primarily observed in the subepithelial basement membrane region of the airway wall and in the adventitia of the airways, with minimal deposition in the lung parenchyma (Fig. 3, B–D).

Morphometric analysis of the total area of collagen deposition in lung tissue sections confirmed these changes (Fig. 3E). There was a trend toward increased subepithelial collagen (by 27%; $P = 0.08$) in the airways of saline-treated *Rxfp1*$^{-/-}$ mice compared with that measured in saline-treated *Rxfp1*$^{+/+}$ mice, whereas OVA treatment of *Rxfp1*$^{+/+}$ and *Rxfp1*$^{-/-}$ mice resulted in an approximately 2-fold increase in collagen deposition (both $P < 0.01$ *vs.* respective saline-treated controls; Fig. 3E), with no differences seen between the OVA-treated *Rxfp1*$^{+/+}$ and *Rxfp1*$^{-/-}$ mice. Hydroxyproline analysis of total lung collagen content (Fig. 3F) reflected what was observed by histological examination. The lungs of saline-treated *Rxfp1*$^{-/-}$ mice had significantly increased lung collagen content (by ~30%; $P < 0.05$) compared with that measured in saline-treated *Rxfp1*$^{+/+}$ mice, whereas OVA treatment of *Rxfp1*$^{+/+}$ and *Rxfp1*$^{-/-}$ mice resulted in an approximately 2-fold increase in total lung collagen content (both $P < 0.01$ *vs.* respective saline-treated controls; Fig. 3F), with no differences observed between OVA-treated *Rxfp1*$^{+/+}$ and *Rxfp1*$^{-/-}$ mice.

Similar changes in collagen subtypes (I, III, and V) were also detected by SDS-PAGE (Fig. 3G) in the four groups studied. The mouse lung was predominantly composed of type I collagen monomers [α1(I) and α2(I) subunits] and dimers (β11 and β12) but lower amounts of type III [α1(III)] and type V [α1(V) and α2(V)] collagen monomers were also detected. The increase in collagen types I, III, and V paralleled the changes seen with total collagen. For example, type I collagen levels in saline-treated *Rxfp1*$^{-/-}$ and OVA-treated mice were about 1.4-fold higher ($P < 0.05$) and 2.2-fold higher (both OVA groups $P < 0.01$), respectively, than that measured in saline-treated *Rxfp1*$^{+/+}$ mice (Fig. 3G). However, as demonstrated for total and subepithelial collagen deposition, the levels of collagen I (Fig. 3G) and the other interstitial collagen subtypes measured were equivalent in OVA-treated *Rxfp1*$^{+/+}$ and *Rxfp1*$^{-/-}$ mice.

To determine whether the elevation in collagen staining (Fig. 3, B–E), content (Fig. 3F), and subtypes (Fig. 3G) was associated with an increased differentiation of airway myofibroblasts, Western blotting of α-SMA expression in lung tissues from the four groups studied was additionally performed (Fig. 3H). A strong correlation was found between increased α-SMA expression, collagen deposition, and collagen subtypes, such that α-SMA expression in saline-treated *Rxfp1*$^{-/-}$ and OVA-treated mice were about 20% higher ($P < 0.05$) and 2-fold higher (both OVA groups $P < 0.01$), respectively, than that measured in saline-treated *Rxfp1*$^{+/+}$ mice (Fig. 3H). Again, the expression of α-SMA was equivalent in OVA-treated *Rxfp1*$^{+/+}$ and *Rxfp1*$^{-/-}$ mice.

Analysis of MMP and TIMP expression and activity in saline- and OVA-treated *Rxfp1*$^{+/+}$ and *Rxfp1*$^{-/-}$ mice

Gelatin zymography of lung tissue from saline- and OVA-treated *Rxfp1*$^{+/+}$ and *Rxfp1*$^{-/-}$ mice was used to assess changes

Downloaded from endo.endojournals.org by on May 31, 2010

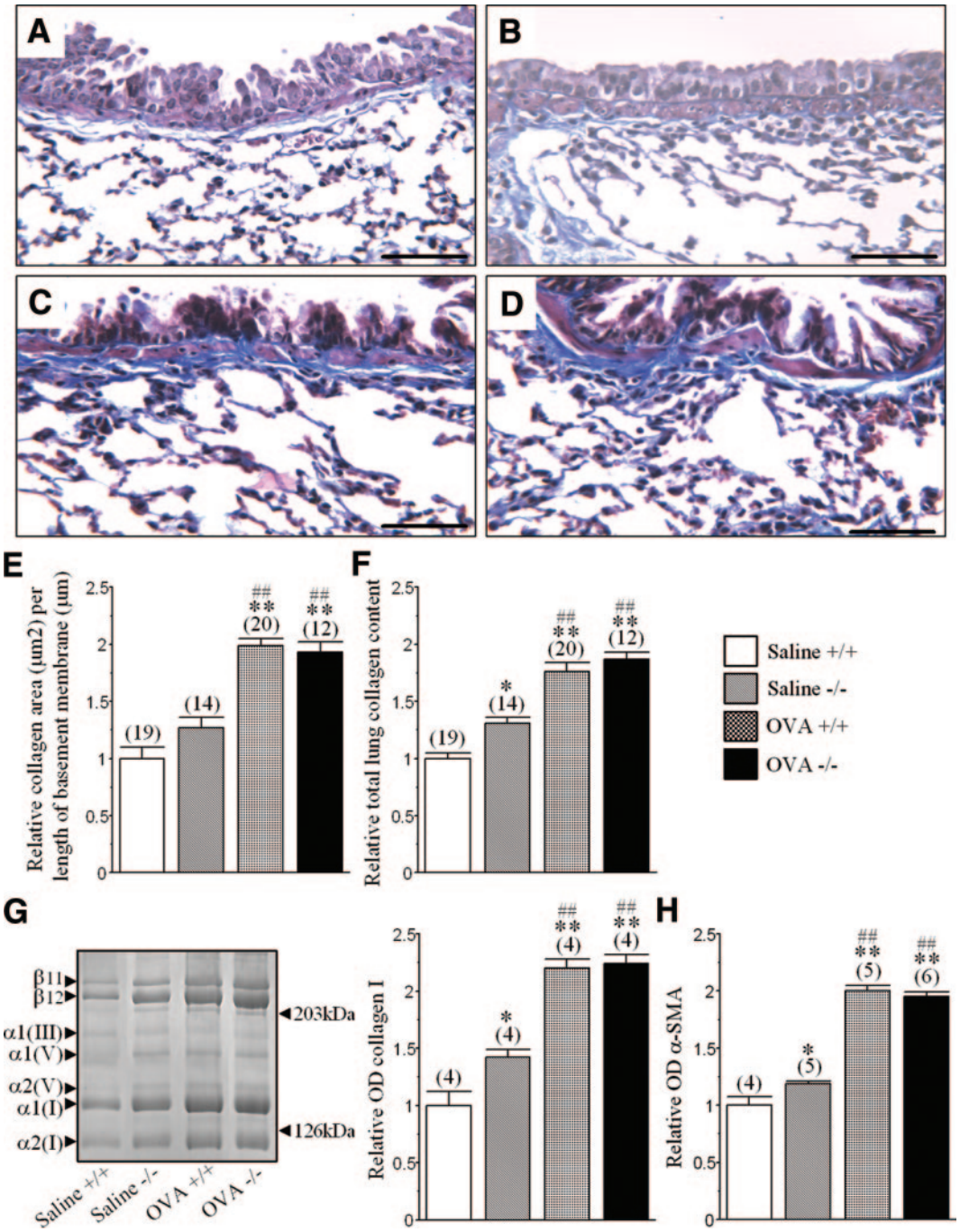

FIG. 3. Histological, morphometric, and biochemical assessment of airway fibrosis and other structural changes in the airways/lung of *Rxfp1*$^{+/+}$ and *Rxfp1*$^{-/-}$ mice. A–D, Masson trichrome-stained lung tissue sections were examined to assess collagen distribution in saline-treated *Rxfp1*$^{+/+}$ (A) and *Rxfp1*$^{-/-}$ (B) mice and OVA-treated *Rxfp1*$^{+/+}$ (C) and *Rxfp1*$^{-/-}$ (D) animals. *Bar*, 100 μm. E–H, The relative mean ± SE subepithelial collagen area (square micrometers) per length basement membrane (micrometers), determined by morphometric analysis (E); total lung collagen content, determined by hydroxyproline assay (F); interstitial collagen subtypes, determined by SDS-PAGE (G); and lung α-SMA content, determined by Western blotting (H) in saline- and OVA-treated *Rxfp1*$^{+/+}$ and *Rxfp1*$^{-/-}$ mice. *Numbers in parentheses* represent number of animals per group. *, $P < 0.05$; **, $P < 0.01$ *vs.* respective values from saline-treated *Rxfp1*$^{+/+}$ mice; ##, $P < 0.01$ *vs.* respective values from saline-treated *Rxfp1*$^{-/-}$ mice.

in gelatinase-A (MMP-2) and gelatinase-B (MMP-9) expression and activity. In each case, no gender-based differences in gelatinase expression/activity were observed, and hence, all results shown are presented as the combined (male and female) data from the four groups studied. Densitometric analysis of the zymographs demonstrated a significant reduction in MMP-9 expression and activity in saline-treated *Rxfp1*$^{-/-}$ mice ($P < 0.05$) and OVA-treated *Rxfp1*$^{+/+}$ and *Rxfp1*$^{-/-}$ animals (both $P <$ 0.01) compared with that measured in saline-treated *Rxfp1*$^{+/+}$ mice (Fig. 4A). MMP-2 expression and activity were also decreased in OVA-treated *Rxfp1*$^{+/+}$ and *Rxfp1*$^{-/-}$ animals (both $P < 0.05$) compared with levels found in saline-treated *Rxfp1*$^{+/+}$ mice (Fig. 4B). The reduction in gelatinase expression and activity was associated with an OVA-induced increase in TIMP-1 expression in *Rxfp1*$^{+/+}$ mice ($P < 0.05$ *vs.* saline-treated *Rxfp1*$^{+/+}$ mice), which was further enhanced in *Rxfp1*$^{-/-}$ an-

Downloaded from endo.endojournals.org by on May 31, 2010

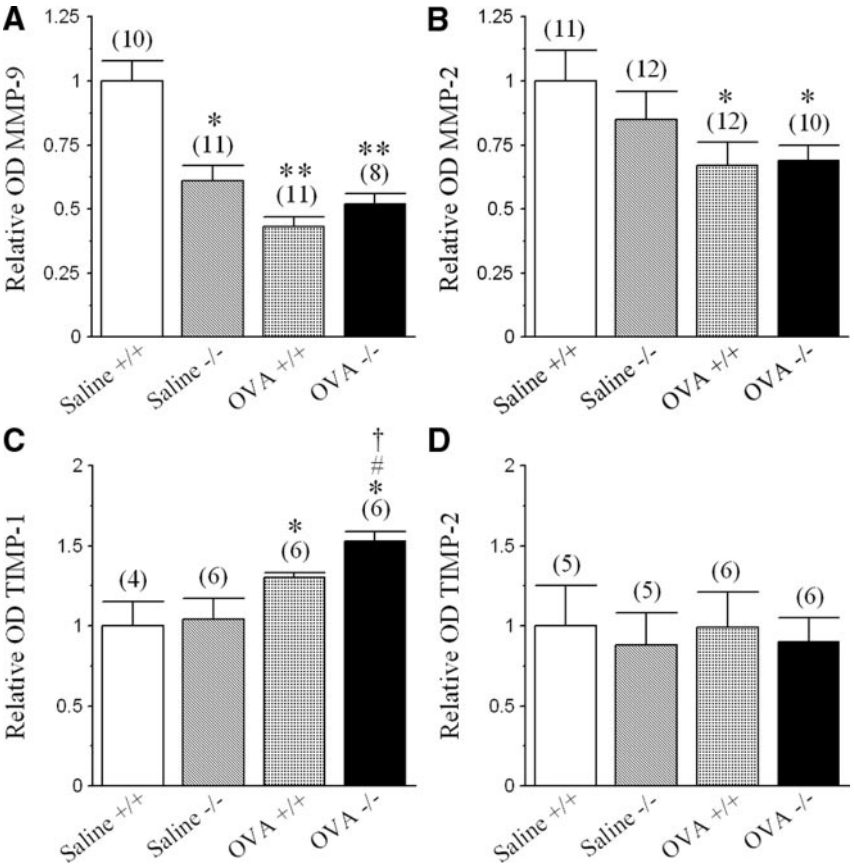

FIG. 4. MMP and TIMP levels in lung tissue of saline- and OVA-treated *Rxfp1*$^{+/+}$ and *Rxfp1*$^{-/-}$ mice. Data are presented as the relative mean ± SE. A–D, MMP-9 (A), MMP-2 (B), TIMP-1 (C), and TIMP-2 (D) levels in saline- and OVA-treated *Rxfp1*$^{+/+}$ and *Rxfp1*$^{-/-}$ mice. *Numbers in parentheses* represent number of animals per group. *, $P < 0.05$; **, $P < 0.01$ *vs.* respective values from saline-treated *Rxfp1*$^{+/+}$ mice; #, $P < 0.05$ *vs.* respective values from saline-treated *Rxfp1*$^{-/-}$ mice; †, $P < 0.05$ *vs.* respective values from OVA-treated *Rxfp1*$^{+/+}$ mice. OD, Optional density.

imals ($P < 0.05$ *vs.* OVA-treated *Rxfp1*$^{+/+}$ and saline-treated mice) (Fig. 4C), whereas no changes in TIMP-2 expression were observed between the four groups studied (Fig. 4D).

Assessment of lung function in saline- and OVA-treated *Rxfp1*$^{+/+}$ and *Rxfp1*$^{-/-}$ mice

Both saline-treated *Rxfp1*$^{+/+}$ and *Rxfp1*$^{-/-}$ animals exhibited standard responses to MCh that were not significantly different from each other (Fig. 5). Both groups of OVA-treated mice developed increased reactivity to MCh, with an increased gradient in the dose-response curves (both $P < 0.001$) as compared with values obtained from respective saline-treated animals (Fig. 5). However, AHR in OVA-treated *Rxfp1*$^{-/-}$ mice was equivalent to that in OVA-treated *Rxfp1*$^{+/+}$ animals. Therefore, the increased airway reactivity seen in OVA-treated animals was related to the presence of AAD and was not influenced by the absence of RXFP1.

Discussion

In this study, a number of important findings were demonstrated. First, RXFP1 appeared to play an important role in the homeostatic regulation of airway fibrosis (because young, saline-treated *Rxfp1*$^{-/-}$ mice underwent increased airway myofibroblast differentiation and collagen deposition, in addition to a reduction in MMP-9 expression and activity compared with that measured in saline-treated *Rxfp1*$^{+/+}$ animals). The fact that this age-related collagen deposition in the airways/lung occurs much earlier in *Rxfp1*$^{-/-}$ mice (17) compared with *Rln*$^{-/-}$ animals may reflect differences in their genetic background (strain) or the possibility that molecules other than relaxin (18) may also signal through RXFP1 to regulate homeostatic airway/lung collagen deposition. Second, consistent with our previous findings for the model of AAD (6, 20), long-term OVA treatment of *Rxfp1*$^{+/+}$ and *Rxfp1*$^{-/-}$ mice resulted in these animals having a marked increase in collagen deposition and airway fibrosis (which was associated with an ~2-fold increase in both airway myofibroblast differentiation and collagen deposition, a significant reduction in MMP-2 and -9 expression and activity, an ~1.5-fold elevation in TIMP-1 expression, and a significant increase in AHR). Third, RXFP1 did not appear to play a significant role in airway fibrosis associated with AAD (because RXFP1 deficiency did not lead to modulation of the degree of myofibroblast differentiation, collagen deposition, gelatinase expression, and activity or AHR induced by AAD compared with that measured from OVA-treated *Rxfp1*$^{+/+}$ animals). This latter observation is the most remarkable finding of this study and suggests that 1) RXFP1 does not mediate the protective effects of relaxin against inflammation-induced airway fibrosis and 2) that relaxin is po-

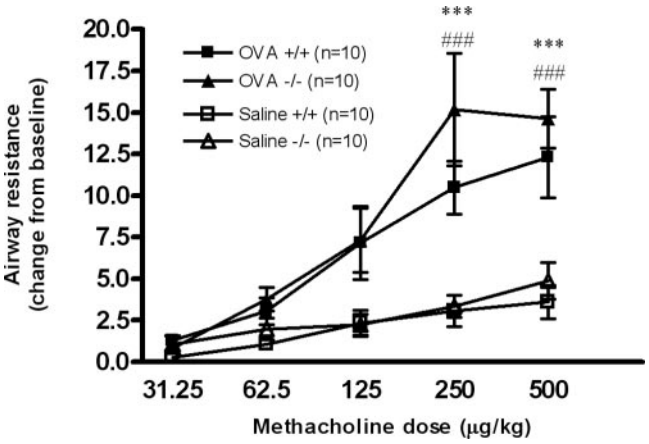

FIG. 5. MCh-induced airway responses in saline- and OVA-treated *Rxfp1*$^{+/+}$ and *Rxfp1*$^{-/-}$ mice. Airway reactivity was measured using invasive plethysmography (n = 10 animals per group) and expressed as maximal resistance after each dose of MCh minus baseline (saline alone) resistance. ***, $P < 0.001$ *vs.* respective values from saline-treated *Rxfp1*$^{+/+}$ mice; ###, $P < 0.001$ *vs.* respective values from saline-treated *Rxfp1*$^{-/-}$ mice.

Downloaded from endo.endojournals.org by on May 31, 2010

tentially working through an alternative receptor to induce its protective effects against inflammation-induced fibrosis [because OVA-treated $Rln^{-/-}$ mice demonstrated significantly higher airway collagen deposition (fibrosis), compared with OVA-treated $Rln^{+/+}$ animals (6)]. It is possible that the effects of relaxin in the setting of inflammation may be mediated by the glucocorticoid receptor because relaxin has been shown to act as an agonist for this receptor (19), which is widely expressed in the respiratory tract (29) and has been extensively studied as a therapeutic target for the treatment of AADs (29–31).

Deficiency of RXFP1 in the resting state (in saline-treated $Rxfp1^{-/-}$ mice) was associated with a significant reduction in MMP-9 activity and increased collagen deposition in the airways but did not affect MMP-2, TIMP-1, or TIMP-2 expression compared with that measured in wild-type mice. This suggests that RXPF1 is an important regulator of collagen deposition and fibrosis during homeostasis and mediates its protective effects at least in part through up-regulation of MMP-9. The demonstration that RXFP1 knockout mice have a more rapid onset of airway/lung fibrosis (17) compared with that measured in age-matched relaxin-deficient animals (6) further suggests that RXFP1 plays a greater role in protecting against fibrosis during homeostasis than relaxin and that other ligands in addition to relaxin may activate the RXFP1 receptor to regulate the balance of extracellular matrix deposition/degradation in the healthy state.

An important finding in this study was that RXFP1 deficiency did not affect collagen deposition, α-SMA, MMP-9, MMP-2, or TIMP-2 in the presence of inflammation (AAD), with expression levels being equivalent to those in wild-type mice with AAD. Furthermore, although OVA-treated RXFP1-deficient mice demonstrated a modest but significant increase in TIMP-1 expression (above that measured in OVA-treated wild-type animals), this increase in TIMP-1 did not result in a corresponding increase in subepithelial or total collagen. These findings suggest that RXPF1 is not a major regulator of MMP-9, MMP-2, TIMP-2, and collagen deposition in the setting of airway inflammation and that TIMP-1 does not play a major role in the progression of inflammation-induced airway fibrosis and/or other factors may counteract the profibrotic effects of TIMP-1 in the setting of inflammation in AAD. Moreover, both the OVA-treated RXFP1-deficient and wild-type mice demonstrated reduced MMP-9 and MMP-9/TIMP-1 ratio as has been previously reported in mice with AAD (32) and asthmatic humans (33, 34), indicating that the regulation of MMP-9 and inflammation-induced airway fibrosis is not predominantly mediated through RXFP1.

In contrast to these findings for RXFP1, relaxin has been shown to play an important role in protecting against airway fibrosis during inflammation (AAD) that is mediated in part through MMP-9 and MMP-2. OVA-treated relaxin-deficient mice had significantly exaggerated airway fibrosis, reduced MMP-9 activity, and a failure to up-regulate MMP-2 levels (6) compared with relaxin wild-type mice with AAD. The lack of an effect of RXFP1 in the setting of AAD suggests that relaxin may signal through other receptor systems to regulate inflammation-induced fibrosis.

One caveat of our current study is that although the relaxin- and RXFP1-knockout mice are on similar backgrounds [*i.e.* C57BL/6J × 129sv (13) *vs.* C57BL/6 (albino) × 129sv (16), respectively], it is possible that minor strain differences may have contributed to the more rapid progression of fibrosis in the $Rxfp1^{-/-}$ mice. However, we believe that minor strain differences are unlikely to account for this finding because airway fibrosis has been shown to be similar in $Rxfp1^{-/-}$ mice on at least two different genetic backgrounds (17). Nevertheless, further work is required to compare the effects of relaxin *vs.* RXFP1 deficiency on the same background and generation of mice to confirm our present findings.

In summary, our findings suggest a paradigm whereby RXFP1 mediates regulation of fibrosis during the homeostatic state (17) rather than inflammation-associated fibrosis, whereas relaxin appears to play a role in both homeostatic (4, 5) and inflammation-associated fibrosis (6), with a greater role in the latter. Further work is now required to determine which putative receptors relaxin might be signaling through to mediate its protective effects against airway fibrosis associated with AAD. Although it has been demonstrated that rodent relaxin is not a native ligand for the rodent insulin-like peptide 3 receptor, RXFP2 (35), human gene-2 (H2) relaxin can activate this receptor, raising this as a potential receptor pathway for relaxin-induced effects in the setting of inflammation. The possibility that relaxin may mediate its protective effects in the inflamed lung through activation of the glucocorticoid receptor (19) or receptors involved in tyrosine kinase signaling (36), which are widely distributed in the airways/lung and play important roles in the prevention of AADs, including asthma, should also be addressed.

Acknowledgments

We sincerely thank Ms. Chongxin Zhao for technical assistance.

Address all correspondence and requests for reprints to: Assoc. Prof. Mimi Tang, Department of Allergy and Immunology, Royal Children's Hospital or Dr. Chrishan Samuel, University of Melbourne, Parkville 3052, Australia. E-mail: mimi.tang@mcri.edu.au or chrishan.samuel@florey.edu.au.

This study was supported by a National Heart Foundation of Australia/National Health and Medical Research Council of Australia (NHMRC) R.D. Wright Fellowship to C.S.S., Salary Support Grants from the Murdoch Children's Research Institute to S.G.R., and M.L.K.T., and a NHMRC Senior Principal Research Fellowship to G.W.T.

Disclosure Statement: All authors have nothing to declare.

References

1. **Bathgate RA, Hsueh AJ, Sherwood OD** 2006 Physiology and molecular biology of the relaxin peptide family. In: Knobil E, Neill JD, eds. Physiology of reproduction. 3rd ed. San Diego: Elsevier; 679–770
2. **Sherwood OD** 2004 Relaxin's physiological roles and other diverse actions. Endocr Rev 25:205–234
3. **Bryant-Greenwood GD, Schwabe C** 1994 Human relaxins: chemistry and biology. Endocr Rev 15:5–26
4. **Samuel CS, Zhao C, Bathgate RA, Du XJ, Summers RJ, Amento EP, Walker LL, McBurnie M, Zhao L, Tregear GW** 2005 The relaxin gene-knockout mouse: a model of progressive fibrosis. Ann NY Acad Sci 1041:173–181

Downloaded from endo.endojournals.org by on May 31, 2010

5. **Samuel CS, Zhao C, Bathgate RA, Bond CP, Burton MD, Parry LJ, Summers RJ, Tang ML, Amento EP, Tregear GW** 2003 Relaxin deficiency in mice is associated with an age-related progression of pulmonary fibrosis. FASEB J 17:121–123
6. **Mookerjee I, Solly NR, Royce SG, Tregear GW, Samuel CS, Tang ML** 2006 Endogenous relaxin regulates collagen deposition in an animal model of allergic airway disease. Endocrinology 147:754–761
7. **Samuel CS, Royce SG, Burton MD, Zhao C, Tregear GW, Tang ML** 2007 Relaxin plays an important role in the regulation of airway structure and function. Endocrinology 148:4259–4266
8. **Unemori EN, Pickford LB, Salles AL, Piercy CE, Grove BH, Erikson ME, Amento EP** 1996 Relaxin induces an extracellular matrix-degrading phenotype in human lung fibroblasts in vitro and inhibits lung fibrosis in a murine model in vivo. J Clin Invest 98:2739–2745
9. **Bani D, Ballati L, Masini E, Bigazzi M, Sacchi TB** 1997 Relaxin counteracts asthma-like reaction induced by inhaled antigen in sensitized guinea pigs. Endocrinology 138:1909–1915
10. **Kenyon NJ, Ward RW, Last JA** 2003 Airway fibrosis in a mouse model of airway inflammation. Toxicol Appl Pharmacol 186:90–100
11. **Hsu SY, Nakabayashi K, Nishi S, Kumagai J, Kudo M, Sherwood OD, Hsueh AJ** 2002 Activation of orphan receptors by the hormone relaxin. Science 295: 671–674
12. **Bathgate RA, Ivell R, Sanborn BM, Sherwood OD, Summers RJ** 2006 International Union of Pharmacology LVII: recommendations for the nomenclature of receptors for relaxin family peptides. Pharmacol Rev 58:7–31
13. **Zhao L, Roche PJ, Gunnersen JM, Hammond VE, Tregear GW, Wintour EM, Beck F** 1999 Mice without a functional relaxin gene are unable to deliver milk to their pups. Endocrinology 140:445–453
14. **Zhao L, Samuel CS, Tregear GW, Beck F, Wintour EM** 2000 Collagen studies in late pregnant relaxin null mice. Biol Reprod 63:697–703
15. **Samuel CS, Tian H, Zhao L, Amento EP** 2003 Relaxin is a key mediator of prostate growth and male reproductive tract development. Lab Invest 83: 1055–1067
16. **Krajnc-Franken MA, van Disseldorp AJ, Koenders JE, Mosselman S, van Duin M, Gossen JA** 2004 Impaired nipple development and parturition in LGR7 knockout mice. Mol Cell Biol 24:687–696
17. **Kamat AA, Feng S, Bogatcheva NV, Truong A, Bishop CE, Agoulnik AI** 2004 Genetic targeting of relaxin and Insl3 receptors in mice. Endocrinology 145: 4712–4720
18. **Bathgate RAD, Lin F, Hanson NF, Otvos Jr L, Guidolin A, Giannakis C, Bastiras S, Layfield SL, Ferraro T, Mas S, Zhao C, Gundlach AL, Samuel CS, Tregear GW, Wade JD** 2006 Relaxin-3: improved synthesis strategy and demonstration of its high affinity interaction with the relaxin receptor LGR7 both in vitro and in vivo. Biochemistry 45:1043–1053
19. **Dschietzig T, Bartsch C, Stangl V, Baumann G, Stangl K** 2004 Identification of the pregnancy hormone relaxin as glucocorticoid receptor agonist. FASEB J 18:1536–1538
20. **Locke NR, Royce SG, Wainewright JS, Samuel CS, Tang ML** 2007 Comparison of airway remodeling in acute, subacute, and chronic models of allergic airways disease. Am J Respir Cell Mol Biol 36:625–632
21. **Fiscus LC, Van Herpen J, Steeber DA, Tedder TF, Tang ML** 2001 L-Selectin is required for the development of airway hyperresponsiveness but not airway inflammation in a murine model of asthma. J Allergy Clin Immunol 107: 1019–1024
22. **Bergman I, Loxley R** 1963 Two improved and simplified methods for the spectrophotometric determination of hydroxyproline. Anal Chem 35:1961–1965
23. **Samuel CS, Butkus A, Coghlan JP, Bateman JF** 1996 The effect of relaxin on collagen metabolism in the nonpregnant rat pubic symphysis: the influence of estrogen and progesterone in regulating relaxin activity. Endocrinology 137: 3884–3890
24. **Gallop PM, Paz MA** 1975 Posttranslational protein modifications, with special attention to collagen and elastin. Physiol Rev 55:418–487
25. **Sykes B, Puddle B, Francis M, Smith R** 1976 The estimation of two collagens from human dermis by interrupted gel electrophoresis. Biochem Biophys Res Commun 72:1472–1480
26. **Samuel CS, Sakai LY, Amento EP** 2003 Relaxin regulates fibrillin 2, but not fibrillin 1, mRNA and protein expression by human dermal fibroblasts and murine fetal skin. Arch Biochem Biophys 411:47–55
27. **Woessner Jr JF** 1995 Quantification of matrix metalloproteinases in tissue samples. Methods Enzymol 248:510–528
28. **Jeyabalan A, Kerchner LJ, Fisher MC, McGuane JT, Doty KD, Conrad KP** 2006 Matrix metalloproteinase-2 activity, protein, mRNA, and tissue inhibitors in small arteries from pregnant and relaxin-treated nonpregnant rats. J Appl Physiol 100:1955–1963
29. **Barnes PJ** 2004 Distribution of receptor targets in the lung. Proc Am Thorac Soc 1:345–351
30. **Barnes PJ** 2006 Corticosteroid effects on cell signalling. Eur Respir J 27:413–426
31. **Pujols L, Mullol J, Torrego A, Picado C** 2004 Glucocorticoid receptors in human airways. Allergy 59:1042–1052
32. **Lee KS, Jin SM, Lee H, Lee YC** 2004 Imbalance between matrix metalloproteinase-9 and tissue inhibitor of metalloproteinase-1 in toluene diisocyanate-induced asthma. Clin Exp Allergy 34:276–284
33. **Doherty GM, Kamath SV, de Courcey F, Christie SN, Chisakuta A, Lyons JD, Heaney LG, Ennis M, Shields MD** 2005 Children with stable asthma have reduced airway matrix metalloproteinase-9 and matrix metalloproteinase-9/tissue inhibitor of metalloproteinase-1 ratio. Clin Exp Allergy 35:1168–1174
34. **Vignola AM, Kips J, Bousquet J** 2000 Tissue remodeling as a feature of persistent asthma. J Allergy Clin Immunol 105:1041–1053
35. **Scott DJ, Fu P, Shen PJ, Gundlach A, Layfield S, Riesewijk A, Tomiyama H, Hutson JM, Tregear GW, Bathgate RA** 2005 Characterization of the rat INSL3 receptor. Ann NY Acad Sci 1041:13–16
36. **Bartsch O, Bartlick B, Ivell R** 2001 Relaxin signalling links tyrosine phosphorylation to phosphodiesterase and adenylyl cyclase activity. Mol Hum Reprod 7:799–809

Downloaded from endo.endojournals.org by on May 31, 2010